

P 型调制掺杂 1.3 μm InAs/GaAs 量子点激光器姚中辉^{1,2}, 陈红梅^{2,3,4}, 王拓^{2,5}, 蒋成^{1,2}, 张子旻^{1,2*}¹中国科学技术大学纳米技术与纳米仿生学院, 安徽 合肥 230026;²中国科学院苏州纳米技术与纳米仿生研究所, 江苏 苏州 215123;³青岛翼晨镭硕科技有限公司, 山东 青岛 266000;⁴中国科学院苏州纳米技术与纳米仿生研究所南昌研究院, 江西 南昌 330200;⁵长春理工大学理学院高功率半导体激光国家重点实验室, 吉林 长春 130022

摘要 1.3 μm InAs/GaAs 量子点(QD)激光器基于自身优异的光电特性,有望成为下一代光通信系统所急需的高性能、低成本光源。理论分析了提高量子点材料增益的几种方法,然后利用分子束外延(MBE)分别生长非掺杂、p 型调制掺杂的 8 层高质量的量子点激光器外延结构,并分别制备了量子点激光器。另外,为了抑制量子点激发态与基态的激射竞争,设计并优化了激光器腔面的镀膜工艺。最终实现了 300 μm 超短腔长基态激射的 p 型调制掺杂 1.3 μm InAs/GaAs 的量子点激光器,展示出了其在高速光通信系统应用中的巨大潜力。

关键词 激光器; 量子点; p 型调制掺杂; 分子束外延; 腔面镀膜

中图分类号 TN31

文献标志码 A

doi: 10.3788/CJL202148.1601001

1 引言

近年来,随着物联网、人工智能、大数据等新兴信息技术的蓬勃发展,人类社会对于信息流量的需求与日俱增,给光通信领域带来了前所未有的挑战,也更加迫切地需要高速率、低成本、低能耗的光通信光源^[1-2]。1.3 μm 波段在标准单模光纤中传输时具有低损耗、低色散的特性,是光纤传输的三个“窗口”之一,在中短距离信息传输中占据重要的地位。作为信号发射源的高速半导体激光器是光通信系统中必不可少的重要组成部分,目前商用的 1.3 μm 光通信光源主要是 InP 基的 InGaAsP 或者 InGaAlAs 量子阱(QW)激光器^[3]。但是由于 InP 基 QW 具有较小的能带偏移,导致其温度稳定性较差,故 InGaAlAs/InP QW 激光器的特征温度通常只有 90~110 K,而 InGaAsP/InP QW 激光器的特征温度仅有 60 K^[4]。InP 基材料因其温度稳定性较差,故在工作时需要增加温控系统来保证器件的正常运行,难以满足高速光通信系统中低能耗、低成本的发展需求。而 GaAs 基 QW 激光器在 980 nm 发光波段

时具有高达 0.55 eV 的能带偏移量,故具备很高的温度稳定性,最高能实现超过 300 K 的特征温度^[5]。但是,对于 GaAs 基 QW 激光器,由于晶格匹配问题,其发光波长很难超过 1.2 μm ^[6]。而 GaAs 基 In(Ga)As 自组织量子点(QD)可以实现超过 1.3 μm 的发光^[7],是当前半导体激光器的研究热点之一。由于载流子的三维限制,QD 具有类原子的分立能级和 δ 函数的态密度,QD 激光器有望实现比 QW 激光器更加优越的性能,比如,低阈值电流密度 J 、高温稳定性、低啁啾、高微分增益、高调制速率、高抗光反射等特性^[8-14];QD 激光器可以在无制冷和无光学隔离器的条件下工作,满足高速率、低成本、低功耗的光源需求,是 5G 光通信光源的有力竞争者之一。但是,QD 材料在实际外延生长过程中的 In-Ga 互混效应会导致较浅的限制势能,降低了基态增益,在一定程度上限制了激光器的高速调制能力。此外,在实际制备的 QD 材料中,其空穴能级间隔较小,空穴容易热逃逸到上能级,影响激光器的温度稳定性。近年来,研究表明 p 型调制掺杂可以有效地提高 QD 激光器的性能,不仅可以抑制 In-Ga 互混,缓解载流子热

收稿日期: 2020-12-15; **修回日期:** 2021-01-12; **录用日期:** 2021-01-27

基金项目: 江西省应用研究培育计划资助项目(20181BBE58020)

通信作者: *zyzhang2014@sinano.ac.cn

逃逸^[15-16],而且可以有效地提高载流子的弛豫速率^[17],实现高调制速率、高温稳定性 QD 激光器。对于高速激光器而言,腔长太长会增加光子寿命,导致低的响应速率,而腔长太短容易增益饱和,缩短响应时间^[16],因此制备高饱和增益的短腔 QD 激光器十分关键。最近,柏林工业大学采用 500 μm 腔长的 p 型掺杂 QD 激光器实现了 15 Gbit/s 的传输速率^[18]。日本 QD Laser 公司采用高增益的 QD 外延结构实现了高达 25 Gbit/s 的直接调制速率^[19]。

本研究通过设计优化 1.3 μm QD 外延结构,采用分子束外延(MBE)成功制备了 8 层 p 型调制掺杂的 QD 结构,通过进一步优化 QD 间隔层厚度,在器件腔面无镀膜的条件下实现了 400 μm 腔长基态激射。为了进一步缩短基态激射腔长,基于 $\text{TiO}_2/\text{SiO}_2$ 体系对高反射膜进行设计,使其在基态波段反射率较高而在激发态波段反射率较低。最终仅在器件后腔面镀膜反射膜的条件下实现了 300 μm 超短腔长基态激射,有望实现 25 Gbit/s 的传输速率。

2 实验部分

2.1 外延结构设计及生长

为了实现高速率的直接调制 QD 激光器,需要尽可能地提高激光器的模式增益。QD 激光器的饱和模式增益与 QD 的体密度、光限制因子成正比,与光谱展宽成反比^[20],表达式为

$$G_{\text{sat}} \propto \frac{N_{\text{QD}} n_{\text{QD}} \Gamma}{\Delta}, \quad (1)$$

其中 G_{sat} 是饱和模式增益, N_{QD} 是有源区 QD 的层数, n_{QD} 是有源区单层 QD 的面密度, Γ 是光限制因子, Δ 是 QD 的光谱展宽。因此,提高 QD 激光器的增益可以通过优化 (1) 式中的一种或者几种参数来实现。本研究在保证每层 QD 面密度 ($4.3 \times 10^{10} \text{ cm}^{-2}$) 较高的同时,将 QD 层数提高到 8 层。但随着 QD 层数的增加,应力不断地积累,容易导致较多的缺陷,使材料发光性能降低,因此需要对生长参数进行优化。另一方面, GaAs 间隔层厚度也是十分重要的。间隔层厚度过小时,失配应力过度积累,会导致发光强度降低以及 QD 的均匀性变差。而间隔层的厚度过厚,会导致限制因子减小,降低模式增益^[21],且过厚的间隔层会增加有源区的串联电阻,使器件热效应更加明显。本研究采用 MBE 优化生长参数,在保证控制表面粗糙度的前提下成功地将有源区间隔层控制在 33 nm 左右。

激光器的模式增益随电流注入的关系可以简

写为^[22]

$$G_{\text{mod}} = G_{\text{sat}} (f_c - f_v), \quad (2)$$

其中, G_{mod} 是激光器模式增益, $(f_c - f_v)$ 用于描述跃迁能级对的载流子反转程度, f_c 为导带受激复合能级的电子占据率, f_v 为价带受激复合能级的电子占据率。通常对于 QD 结构,当导带电子能级间隔约为 80 meV 时,价带的空穴能级间隔仅有 10 meV,因此注入的空穴极易热逃逸到上能级,导致大量的注入载流子没有被耦合到有效的发光模式中而被浪费^[16]。而通过在 QD 有源区引入 p 型调制掺杂进行空穴的补偿,可以有效提高空穴在价带基态的占据率,增加基态增益。

采用 MBE 在 Si 掺杂的 GaAs (100) 衬底上分别制备了非掺杂和 p 型调制掺杂的 In(Ga)As/GaAs QD 激光器外延结构。非掺杂和 p 型掺杂 QD 结构的生长条件除掺杂外完全相同,有源区均由 8 层 InAs QD 组成,其中每层 QD 被 33 nm 的 GaAs 间隔层隔开,每层 QD 包含 2.7 ML(monolayer, 单层) InAs 以及 6 nm 的 InGaAs 应力释放层。整个有源区结构置于上下包层之中,其中上包层是约 1800 nm 的 $\text{p-Al}_{0.3}\text{Ga}_{0.7}\text{As}$, 下包层是约 2800 nm 的 $\text{n-Al}_{0.3}\text{Ga}_{0.7}\text{As}$, 最终将 200 nm 的 $\text{p}^+\text{-GaAs}$ 作为电接触层。QD 激光器外延结构示意图如图 1 所示,插图是 QD 有源区的截面透射电子显微镜(TEM)图,从中可以清晰地看到被 33 nm GaAs 层隔开的 8 层 InAs QD。对于 p 型掺杂的 QD 结构,采用 Be 元素进行调制掺杂,宽度为 6 nm 的 Be 掺杂层位于 InAs/InGaAs QD 层以下 10 nm,掺杂 Be 分子浓度为 $3 \times 10^{17} \text{ cm}^{-3}$ 。

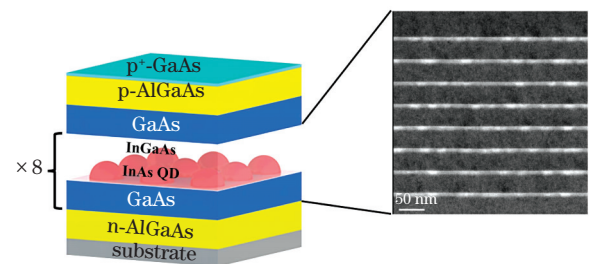


图 1 QD 样品的结构示意图(插图:QD 有源区的 TEM 图)

Fig. 1 Schematic structure of the QD samples

(Inset: TEM image of the QD active region)

2.2 器件设计及制备

采用光刻、干法刻蚀与湿法腐蚀相结合的工艺制备了脊宽为 3.5 μm 的 QD F-P 激光器,如图 2 所示。为了减小器件的寄生电容,采取了球拍型电极。激光器腔面镀膜是调控性能的重要手段之一。激光器的阈值模式增益与腔面反射率符合以下关系,

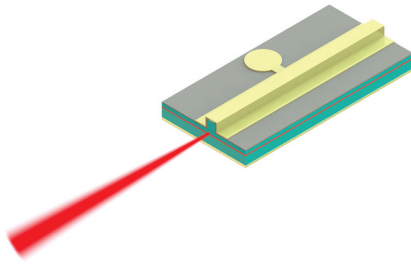


图 2 量子点激光器结构示意图

Fig. 2 Schematic diagram of QD laser structure

$$g_{\text{mod}} = \alpha_i + \frac{1}{2L} \ln [1/(R_1 R_2)], \text{ 其中}$$

$\frac{1}{2L} \ln [1/(R_1 R_2)]$ 代表腔面损耗, R_1 和 R_2 分别是前、后腔面的反射率, α_i 代表内损耗。因此, 对激光器腔面蒸镀高反膜可以减小腔面损耗, 降低激光器的阈值电流, 对腔面起到保护作用^[23]。常用的腔面镀膜技术通常交替生长光学厚度为 $\lambda/4$ 的高低折射率材料, 其中 λ 是激光器的输出激光波长。为了抑制激发态激射, 采用基态高反射率/激发态低反射率的方法, 使用 TiO_2 和 SiO_2 分别作为高低折射率材料, 模拟不同中心波长的反射率曲线, 如图 3 所示。从图中可以看出: 当膜系的中心波长为 1310 nm 时, 基态和激发态的反射率都在 95% 以上; 而当中心波长为 1480 nm 时, 可以看出基态 1310 nm 波段的反射率为 94% 而激发态 1220 nm 波段的反射率为 23%, 符合基态高反射率、激发态低反射率的需求。基于这种设计最终实现了超短腔长 300 μm 基态激射的 1.3 μm QD 激光器。

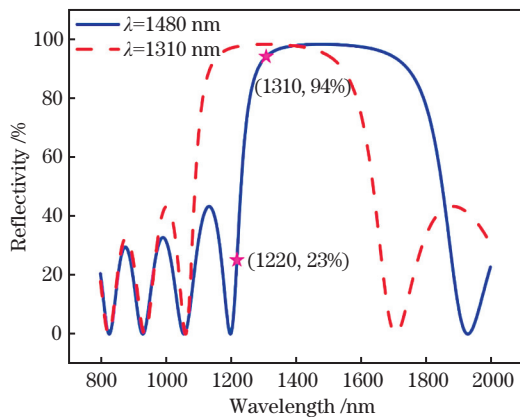


图 3 不同中心波长的反射率模拟谱

Fig. 3 Simulated reflectivity spectra with different central wavelengths

3 分析与讨论

3.1 材料光致发光表征

QD 样品的光致发光 (PL) 谱如图 4 所示, 图中可

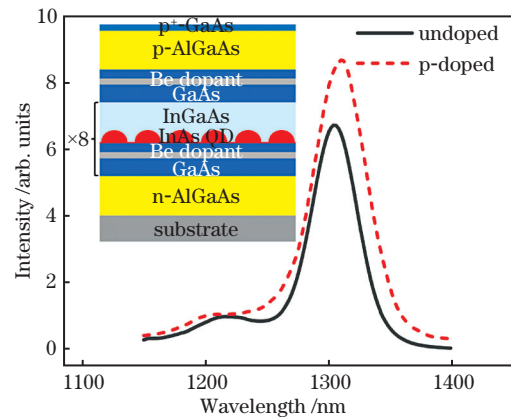


图 4 室温下非掺杂和 p 型掺杂 QD 材料的 PL 谱

Fig. 4 PL spectra measured at room temperature for the undoped and p-doped QD materials

以看出非掺杂 QD 样品的发光峰相对于 p 型掺杂样品有一定程度的蓝移, 这是由于 $\text{p-Al}_{0.3}\text{Ga}_{0.7}\text{As}$ 上包层的生长温度 (600 $^{\circ}\text{C}$) 高于 QD 有源区的生长温度 (500 $^{\circ}\text{C}$), 长时间生长上包层的过程相当于对有源区进行退火, 在此过程中会形成 Ga 原子空位, QD 和周围材料发生 In-Ga 互混, 导致发光峰蓝移^[24]。而 p 型掺杂的引入能够提高间隙原子浓度, 抑制 Ga 空位的产生和转移, 因此能够有效地抑制退火过程中的 In-Ga 互混, 使其发光峰位蓝移程度减小^[25]。从图中还可以看出, 与非掺杂 QD PL 谱比较, p 掺杂 QD 的 PL 谱有一定幅度的展宽。这主要是因为 p 型掺杂产生了较为显著的能态填充效应^[26]。P 型掺杂的引入不仅对材料结构有影响, 而且对 In(Ga)As/GaAs QD 的载流子动力学也有重大的影响。如图 5 所示: p 型掺杂 QD 价带空穴的占据率非常高, 而且, 更重要的是其在退火之后能带结构几乎没有发生变化; 而非掺杂 QD 样品由于在退火过程中具有较强的 In-Ga 互混效应, 材料组分分布变得模糊且能带结构发生明显的变化, 导致其限制势减小, 载流子易逃逸, 因此造成 PL 光谱蓝移且发光强度变弱; p 型掺杂还以多种方式影响载流子的动力学过程。载流子的动力学过程主要包括漂移 (过程 1), 捕获 (过程 2), 扩散 (过程 3), 弛豫 (过程 4) 和热逃逸 (过程 5)。GaAs 间隔层中 p 型掺杂的引入产生了多余的空穴, 空穴通过扩散机制向浸润层和应力缓冲层扩散。QD 周围数量丰富的空穴会带来两个结果: 更多的空穴驻留在 QD 中, 能够增强对空穴的捕获概率; 大量的空穴能够提升载流子散射, 有利于载流子从激发态弛豫到基态, 提高基态的发光效率, 在器件高速调制过程中具有重要的作用^[15]。P 型掺杂的引入, 不仅仅可以有效地抑制在外延生长过程中的 In-Ga 互混, 还可以提高 QD 价带

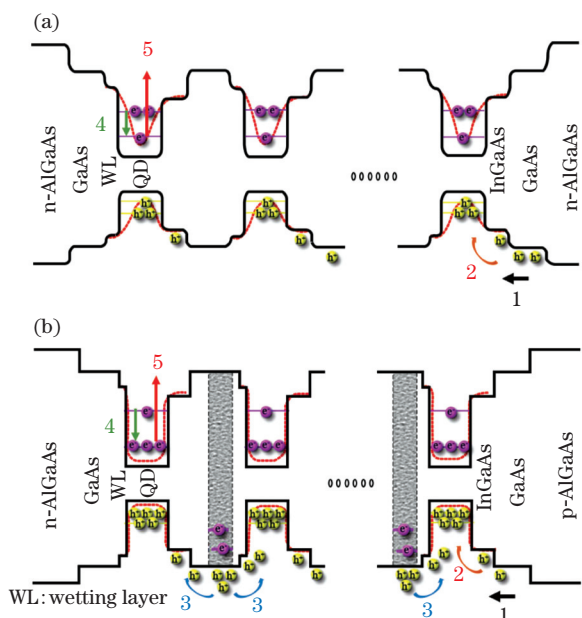


图 5 非掺杂和 p 型掺杂 QD 样品的能带图(虚线代表退火之后的势能曲线)。(a)非掺杂;(b) p 型掺杂

Fig. 5 Energy band diagrams of the undoped and p-doped QD samples (the dashed lines are the potential profiles after annealing). (a) Undoped; (b) p-doped

基态的空穴占据率,有效地提高材料的光学性能。因此,p 型掺杂 QD 材料优异的光学特性有望实现更高性能的激光器器件。

3.2 器件测试及表征

对于高速激光器而言,实现短腔基态激射是提升高速性能的重要手段之一,从材料表征的结果可以预计 p 型掺杂 QD 材料样品具备更加优异的光电特性,因此,分别制备了不同腔长的非掺杂和 p 型掺杂 QD 激光器,并在室温连续电流注入下对其进行测试。图 6 为非掺杂和 p 型掺杂 QD 激光器基态阈

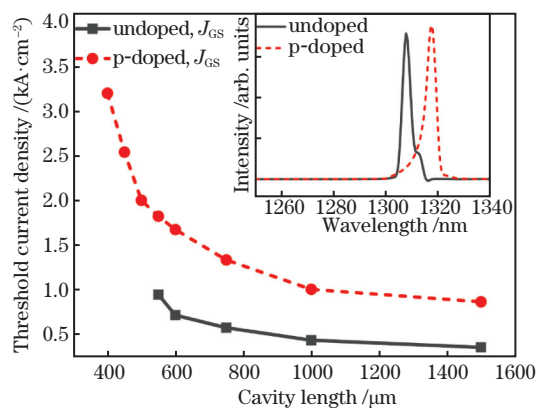


图 6 非掺杂和 p 型掺杂 QD 激光器基态阈值电流密度随器件腔长 L 的变化(插图:非掺杂和 p 型掺杂 QD 激光器激光光谱)

Fig. 6 Cavity length dependence of the threshold current density of ground state for undoped and p-doped QD lasers (Inset: lasing spectra of undoped and p-doped QD lasers)

值电流密度随器件腔长的变化曲线,插图为非掺杂和 p 型掺杂 QD 激光器的激光光谱图。可以看出,非掺杂 QD 激光器最短基态激射腔长为 $550 \mu\text{m}$,而 p 型掺杂可以实现 $400 \mu\text{m}$ 腔长基态激射,这主要是由于 p 型掺杂能够有效地提高基态模式的增益。从图中可以明显看出,非掺杂和 p 型掺杂 QD 激光器均随着腔长的缩短,基态的阈值电流密度 J_{GS} 逐渐升高,这主要是由于腔长的缩短使腔面损耗增加所致。相比于非掺杂 QD 激光器,p 型掺杂激光器的阈值电流密度更高,这主要是因为 p 型掺杂引入了非辐射复合中心所致。为了进一步缩短腔长,采用如图 3 所述的基态高反射率、激发态低反射率的腔面镀膜方法对 p 型掺杂 QD 激光器进行了腔面镀膜。图 7(a)是中心波长

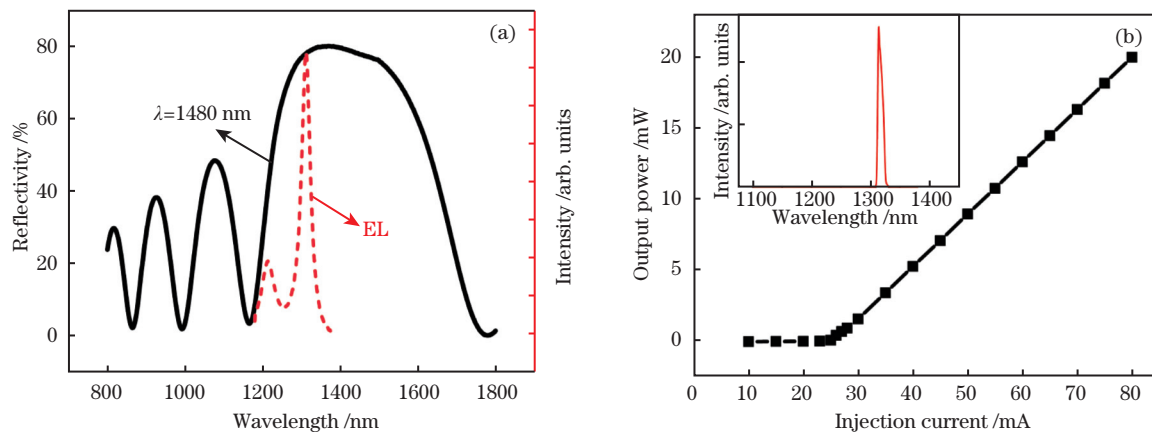


图 7 测试反射谱与 QD 激光器 EL 谱。(a) $\lambda=1480 \text{ nm}$ 的腔面反射率与 p-doped QD 激光器 EL 谱;(b) p-doped QD 激光器 $300 \mu\text{m}$ 腔长镀膜激射谱

Fig. 7 Measured reflectivity spectra and EL of QD laser. (a) Reflectivity spectra with $\lambda=1480 \text{ nm}$ and EL of p-doped QD laser; (b) lasing spectra of $300 \mu\text{m}$ p-doped QD laser with coated

为 1480 nm 的 4 对 $\text{TiO}_2/\text{SiO}_2$ 材料反射率谱与 p 型掺杂 QD 激光器电致发光 (EL) 光谱的对应关系。采用此反射膜设计, 本研究成功地抑制了 QD 激发态激射, 最终实现了超短腔长 300 μm 的基态激射。器件输出功率如图 7(b) 所示, 室温连续注入 80 mA 时, 输出功率达到 20 mW; 器件激射光谱如图 7(b) 插图所示。缩短腔长可以有效地缩短腔内光子寿命、提高调制速率, 相比于德国柏林工业大学采用 500 μm 腔长的 p 型掺杂 QD 激光器实现 15 Gbit/s 的基态调制速率^[18], 300 μm 超短腔长 QD 激光器有望实现更高的调制速率。

4 结 论

通过设计优化 QD 外延结构与生长参数, 成功制备了 GaAs 间隔层为 33 nm 的非掺杂和 p 型掺杂 8 层 QD 激光器材料结构。通过综合分析 PL 光谱, 证实 p 型掺杂可以有效抑制外延生长中 QD 与周围材料的 In-Ga 互混效应, 增强了载流子限制势, 提升了材料的发光性能。基于所生长的两种 QD 材料制备成激光器后, 又进一步证实了 p 型掺杂的优点, 相比非掺杂器件, 在没有镀膜的条件下 p 型掺杂激光器可以实现更短腔长 (400 μm) 的基态激射。为了进一步提升器件的性能, 设计中心波长为 1480 nm, 4 对 $\text{TiO}_2/\text{SiO}_2$ 作为高低折射率材料的反射膜结构, 实现了 300 μm 超短腔长基态激射的 p 型掺杂 QD 激光器, 其在高速调制方面表现出了巨大的潜力。

参 考 文 献

- [1] Lü Z R, Zhang Z K, Wang H, et al. Research progress on 1.3 μm semiconductor quantum-dot lasers[J]. Chinese Journal of Lasers, 2020, 47(7): 0701016.
吕尊仁, 张中恺, 王虹, 等. 1.3 μm 半导体量子点激光器的研究进展[J]. 中国激光, 2020, 47(7): 0701016.
- [2] Sun C Z, Yang S H, Xiong B, et al. Progress in high-speed electroabsorption modulated lasers [J]. Chinese Journal of Lasers, 2020, 47(7): 0701002.
孙长征, 杨舒涵, 熊兵, 等. 高速电吸收调制激光器研究进展[J]. 中国激光, 2020, 47(7): 0701002.
- [3] Lu D, Yang Q L, Wang H, et al. Review of semiconductor distributed feedback lasers in the optical communication band [J]. Chinese Journal of Lasers, 2020, 47(7): 0701001.
陆丹, 杨秋露, 王皓, 等. 通信波段半导体分布反馈激光器[J]. 中国激光, 2020, 47(7): 0701001.
- [4] Zhukov A E, Kovsh A R. Quantum dot diode lasers for optical communication systems [J]. Quantum Electronics, 2008, 38(5): 409-423.
- [5] Schäfer F, Mayer B, Reithmaier J P, et al. High-temperature properties of GaInAs/AlGaAs lasers with improved carrier confinement by short-period superlattice quantum well barriers [J]. Applied Physics Letters, 1998, 73(20): 2863-2865.
- [6] Sato S, Satoh S. 1.21 μm continuous-wave operation of highly strained GaInAs quantum well lasers on GaAs substrates [J]. Japanese Journal of Applied Physics, 1999, 38(9A): L990-L992.
- [7] Huffaker D L, Park G, Zou Z, et al. 1.3 μm room-temperature GaAs-based quantum-dot laser [J]. Applied Physics Letters, 1998, 73(18): 2564-2566.
- [8] Arakawa Y, Sakaki H. Multidimensional quantum well laser and temperature dependence of its threshold current [J]. Applied Physics Letters, 1982, 40(11): 939-941.
- [9] Li Q Z, Huang Y Q, Ning J Q, et al. InAs/GaAs quantum dot dual-mode distributed feedback laser towards large tuning range continuous-wave terahertz application [J]. Nanoscale Research Letters, 2018, 13(1): 267.
- [10] Fathpour S, Mi Z, Bhattacharya P, et al. The role of Auger recombination in the temperature-dependent output characteristics ($T_0 = \infty$) of p-doped 1.3 μm quantum dot lasers [J]. Applied Physics Letters, 2004, 85(22): 5164-5166.
- [11] Deppe D G, Shavritranuruk K, Ozgur G, et al. Quantum dot laser diode with low threshold and low internal loss [J]. Electronics Letters, 2009, 45(1): 54-56.
- [12] Kageyama T, Takada K, Nishi K, et al. Long-wavelength quantum dot FP and DFB lasers for high temperature applications [J]. Proceedings of SPIE, 2012, 8277: 82770C.
- [13] He Y M, Zhang Z K, Lü Z, et al. 10-Gbps 20-km feedback-resistant transmission using directly modulated quantum-dot lasers [J]. IEEE Photonics Technology Letters, 2020, 32(21): 1353-1356.
- [14] MaXueer X Y, He Y M, Lü Z R, et al. 1.3 μm p-modulation doped InGaAs/GaAs quantum dot lasers with high speed direct modulation rate and strong optical feedback resistance [J]. Crystals, 2020, 10(11): 980-987.
- [15] Li Q Z, Wang X, Zhang Z Y, et al. Development of modulation p-doped 1310 nm InAs/GaAs quantum dot laser materials and ultrashort cavity Fabry-Perot and distributed-feedback laser diodes [J]. ACS

- Photonics, 2018, 5(3): 1084-1093.
- [16] Deppe D G, Huang H, Shchekin O B. Modulation characteristics of quantum-dot lasers: the influence of p-type doping and the electronic density of states on obtaining high speed[J]. IEEE Journal of Quantum Electronics, 2002, 38(12): 1587-1593.
- [17] Gündođdu K, Hall K C, Boggess T F, et al. Ultrafast electron capture into p-modulation-doped quantum dots[J]. Applied Physics Letters, 2004, 85(20): 4570-4572.
- [18] Arsenijević D, Schliwa A, Schmeckebier H, et al. Comparison of dynamic properties of ground- and excited-state emission in p-doped InAs/GaAs quantum-dot lasers [J]. Applied Physics Letters, 2014, 104(18): 181101.
- [19] Tanaka Y, Ishida M, Takada K, et al. 25 Gbps direct modulation in 1.3- μm InAs/GaAs high-density quantum dot lasers [C] // Conference on Lasers and Electro-Optics 2010, May 16–21, 2010, San Jose, California, United States. Washington, D.C.: OSA, 2010: CTuZ1.
- [20] Zhukov A E, Maksimov M V, Kovsh A R. Device characteristics of long-wavelength lasers based on self-organized quantum dots [J]. Semiconductors, 2012, 46(10): 1225-1250.
- [21] Salhi A, Fortunato L, Martiradonna L, et al. Enhanced modal gain of multilayer InAs/InGaAs/GaAs quantum dot lasers emitting at 1300 nm [J]. Journal of Applied Physics, 2006, 100(12): 123111.
- [22] Ji H M, Yang T, Cao Y L, et al. Theoretical analysis of modal gain in p-doped 1.3 μm InAs/GaAs quantum dot lasers [J]. Physica Status Solidi (c), 2009, 6(4): 948-951.
- [23] Cao Y L, Yang T, Xu P F, et al. Delay of the excited state lasing of 1310 nm InAs/GaAs quantum dot lasers by facet coating [J]. Applied Physics Letters, 2010, 96(17): 171101.
- [24] Zhang Z Y, Jiang Q, Luxmoore I J, et al. A p-type-doped quantum dot superluminescent LED with broadband and flat-topped emission spectra obtained by post-growth intermixing under a GaAs proximity cap [J]. Nanotechnology, 2009, 20(5): 055204.
- [25] Cao Q, Yoon S F, Liu C Y, et al. Effects of rapid thermal annealing on optical properties of p-doped and undoped InAs/InGaAs dots-in-a-well structures [J]. Journal of Applied Physics, 2008, 104(3): 033522.
- [26] Kumagai N, Watanabe K, Nakata Y, et al. Optical properties of p-type modulation-doped InAs quantum dot structures grown by molecular beam epitaxy [J]. Journal of Crystal Growth, 2007, 301/302: 805-808.

P-Modulation Doped 1.3- μm InAs/GaAs Quantum Dot Lasers

Yao Zhonghui^{1,2}, Chen Hongmei^{2,3,4}, Wang Tuo^{2,5}, Jiang Cheng^{1,2}, Zhang Ziyang^{1,2*}

¹ School of Nano-Tech and Nano-Bionics, University of Science and Technology of China, Hefei, Anhui 230026, China;

² Suzhou Institute of Nano-Tech and Nano-Bionics, Chinese Academy of Sciences, Suzhou, Jiangsu 215123, China;

³ Qingdao Yichen Leishuo Technology Co., Ltd., Qingdao, Shandong 266000, China;

⁴ Nanchang Research Institute, Suzhou Institute of Nano-Tech and Nano-Bionics, Chinese Academy of Sciences, Nanchang, Jiangxi 330200, China;

⁵ State Key Laboratory of High Power Semiconductor Lasers, Changchun University of Science and Technology, Changchun, Jilin 130022, China

Abstract

Objective 1.3- μm GaAs-based III-V quantum dot (QD) lasers have several advantages over commercial lasers of InP-based III-V quantum well lasers, such as low threshold current density, high quantum efficiency, high-temperature insensitivity, high optical feedback tolerance, and larger modulation bandwidth owing to the three-dimensional quantum confinement effect of carriers. This has made the 1.3- μm GaAs-based QD laser a very promising candidate as a light source for next-generation low-power-consumption, low-cost, small-footprint, and high-speed fiber-optical communication systems. However, the closely spaced energy levels of the confined holes and In-Ga interdiffusion during epitaxial growth for practical QD laser structures make the performance of current devices still far short of expectations. In addition, for high-speed lasers, a short cavity length is crucial because of the significantly reduced photon lifetime, but there is always a trade-off between cavity length and the saturation modal gain. In recent years, introducing p-doping in the active region to optimize the properties of QD materials has attracted extensive interest. p-Doping in III-V QD structures to compensate the thermal escape of carriers leads to

better thermal stability. Modulation p-doping can significantly inhibit Ga vacancy propagation, leading to smaller interdiffusion and a reduced intermixing effect. In 2010, the ground state 25 Gbit/s operation of a 1.3 μm p-doped QD laser was first reported by Tanaka *et al.* Recently, a 15 Gbit/s high-speed 1.3 μm modulation p-doped QD laser has been demonstrated in a 500 μm long QD laser by Arsenijević *et al.* In this work, we further optimize the performance of QD lasers using subtle epitaxial growth and careful structure design.

Methods The InAs/GaAs multiple QD layer structures were grown using molecular beam epitaxy (MBE) on Si-doped GaAs(100) substrates. The QD active region consists of eight stacks of QD layers separated by 33 nm GaAs spacers (Fig. 1). Each QD layer comprises 2.7 monolayer InAs covered with a 6 nm InGaAs strain-reducing layer, and the active layers were sandwiched between the ≈ 2800 nm n-type $\text{Al}_{0.3}\text{Ga}_{0.7}\text{As}$ lower-cladding layer and ≈ 1800 nm p-type $\text{Al}_{0.3}\text{Ga}_{0.7}\text{As}$ upper-cladding layer. The p-doped QD sample was grown sequentially with identical structures, and the modulation p-doping was performed with Be in a 6 nm layer located in the GaAs spacer layer 10 nm beneath each InAs/InGaAs QD layer to obtain a concentration of $3 \times 10^{17} \text{ cm}^{-3}$. For the effective light excitation and photoluminescence (PL) signal collection, the upper p-side AlGaAs cladding layers were etched away using wet etching above the QD active regions. Ridge waveguide (3.5 μm ridge wide) lasers were fabricated using photolithography and dry-wet etching techniques. To prevent lasing from the first excited state of the QD, careful design and a facet-coating process were fully investigated. Finally, 1.3- μm ground state lasing has been found in p-doped InAs/GaAs QD lasers with a 300 μm ultrashort cavity length, which shows great potential in high-speed optical communication systems.

Results and Discussions The PL peak wavelength of the p-doped sample is longer than that of the undoped sample (Fig. 4). The difference in the emission wavelengths between undoped and p-doped samples is caused by the higher temperature needed for the growth of the AlGaAs cladding layer, which is equivalent to a rapid thermal annealing (RTA) process. The QD samples underwent an annealing effect at the higher growth temperature, in which a strong interdiffusion between QDs and surrounding barrier layers occurred with intermixing for undoped sample, resulting in a remarkable blue-shift of the peak position. Introducing the modulation p-doping can significantly inhibit the Ga vacancy propagation, which leads to smaller interdiffusion and a reduced intermixing effect. To be more specific, we employ the scheme depicted to illustrate the role of p-doping in a microscopic view (Fig. 5). As the result of intermixing, the potential profile of the undoped sample is severely altered, while that of the doped sample almost maintains its original profile due to the intermixing inhibition by p-doping. The excess of holes around the QDs leads to two results: more holes residing in the QDs and enhanced capture of holes in the carrier dynamics. Based on the outstanding performance of p-doped QD samples, continuous-wave (CW) ground state lasing has been realized in a 300 μm ultrashort cavity length laser with facet-coating design (Fig. 7). A shorter cavity length can reduce the photon lifetime, which is of great importance to improve the modulation bandwidth of high-speed lasers.

Conclusions In this work, undoped and p-type modulation doping eight-layer QD laser structures with 33 nm GaAs barriers were successfully fabricated using subtle epitaxial growth and careful structure design. By analyzing the PL spectrum, introducing p-doping can inhibit holes' thermal broadening in their closely spaced energy levels and significantly suppress In/Ga interdiffusion between QDs and their surrounding matrix. Because of the superior features of the modulation p-doped QD materials, CW ground state lasing has been realized in p-doped QD lasers with a short cavity length (400 μm) without facet coatings. To prevent lasing from the first excited state of the QD, careful design and a facet-coating process were fully investigated. Finally, 1.3- μm GS lasing has been found in p-doped InAs/GaAs QD lasers with 300 μm ultrashort cavity length, which shows great potential in high-speed optical communication systems.

Key words lasers; quantum dots; p-modulation doping; molecular beam epitaxy; facet coating

OCIS codes 062.2330; 250.5960; 230.5590